Off-Axis Adaptive Optics with Optimal Control : Experimental and Numerical Validation

C. Petit[a], J.-M. Conan[a], C. Kulcsár[b], H.-F. Raynaud[b], T. Fusco[a], J. Montri[a], F. Chemla[c] and D. Rabaud[d]

[a]ONERA, BP 72, 92322 Châtillon, France
[b]Université Paris 13, Institut Galilée, L2TI, 93430 Villetaneuse, France
[c] Observatoire de Paris-Meudon GEPI, 5 place Jules Janssen, 92195 Meudon Cedex, France
[d]Shaktiware, 27 Bd C. Moretti, 13014 Marseille

ABSTRACT

We present a laboratory demonstration of open loop Off-Axis Adaptive Optics with optimal control. The control based on a Minimum Mean Square Error Estimator brings a noticeable performance improvement. The next step will be to close the Off-Axis Adaptive Optics loop with a Kalman based optimal control. While this last experiment is currently under progress, a classic Adaptive Optics loop has already been closed recently with a Kalman based control and experimental results are presented. We also describe the expectable performance of the Kalman based off-axis closed loop thanks to an end-to-end simulator. **Last minute notice:** the Kalman based Off-Axis Adaptive Optics loop has been closed and very first results are given.

1. INTRODUCTION

Classic Adaptive Optics (AO) performance is limited by anisoplanatism effects. Multi-Conjugate AO (MCAO) is a promising concept that should increase significantly the corrected Field of View (FoV). Various theoretical studies have addressed the issue of MCAO optimal control (see[1] and references therein). An open loop Minimum Mean Square Error (MMSE) Estimator (MMSEE) has been derived[2–4] and an original Kalman based closed loop generalization has been proposed. [1] Still, few experimental validations of the MCAO concept and its control solution have been performed up to now. [5–8] In this article, the open loop MMSEE control is implemented on an Off-Axis Adaptive Optics (OAAO) experimental set-up. This set-up allows to test optimal reconstruction methods in a simplified MCAO configuration. Thus, it will be used to test the Kalman based closed loop control.[9] This new control system is currently being tested and preliminary results, both experimental and numerical, are already presented.

We first describe in Sect.2 the concept of OAAO and the optimal reconstructor used in the context of open loop OAAO. We present the OAAO set-up, and discuss in Sect. 3 the open loop experimental results compared to those provided by an accurate end-to-end simulation. Then we introduce in Sect. 4 the Kalman based optimal control that will perform optimal closed loop OAAO. Its implementation on the set-up is presented shortly. A classic AO loop has been already closed with this optimal control and first results are discussed. Looking forward to closing the loop in off-axis correction, a simulation of the Kalman based closed loop OAAO expectable performance is already proposed. We finally discuss in Sect. 5 the various applications of this optimal control solution. **Last minute notice:** the Kalman based Off-Axis Adaptive Optics loop has been closed and very first results are given in Sect.7.

2. OAAO AND MMSEE OPTIMAL CONTROL

2.1. OAAO: a simplified MCAO experiment

In MCAO multiple guide stars (GSs) and multiple Wave Front Sensors (WFSs) are used to probe and reconstruct the turbulence in the volume. Then, multiple Deformable Mirrors (DMs) are used to perform the correction in a given FoV of interest. OAAO, described in Fig. 2, is an intermediate concept between MCAO and classic AO. We consider a single turbulent layer at altitude h and two stars with an angular separation α. The on-axis GS is used to analyze the

Further author information: (Send correspondence to Petit Cyril)
Petit Cyril: E-mail: cyril.petit@onera.fr

Astronomical Adaptive Optics Systems and Applications II, edited by Robert K. Tyson, Michael Lloyd-Hart,
Proceedings of SPIE Vol. 5903, 59030P, (2005) · 0277-786X/05/$15 · doi: 10.1117/12.618266

on-axis turbulence. From these measurements, the off-axis turbulent wavefront is estimated and corrected by a single DM, conjugated with the entrance pupil of diameter *D*.

We will first focus on the open loop control, meaning no feedback is performed, only feed-forward. So as to get rid of temporal error, we will also suppress temporal delay in our control by considering a static turbulence. Nevertheless, different occurrences of turbulence will be used so as to obtain statistically meaningful results.

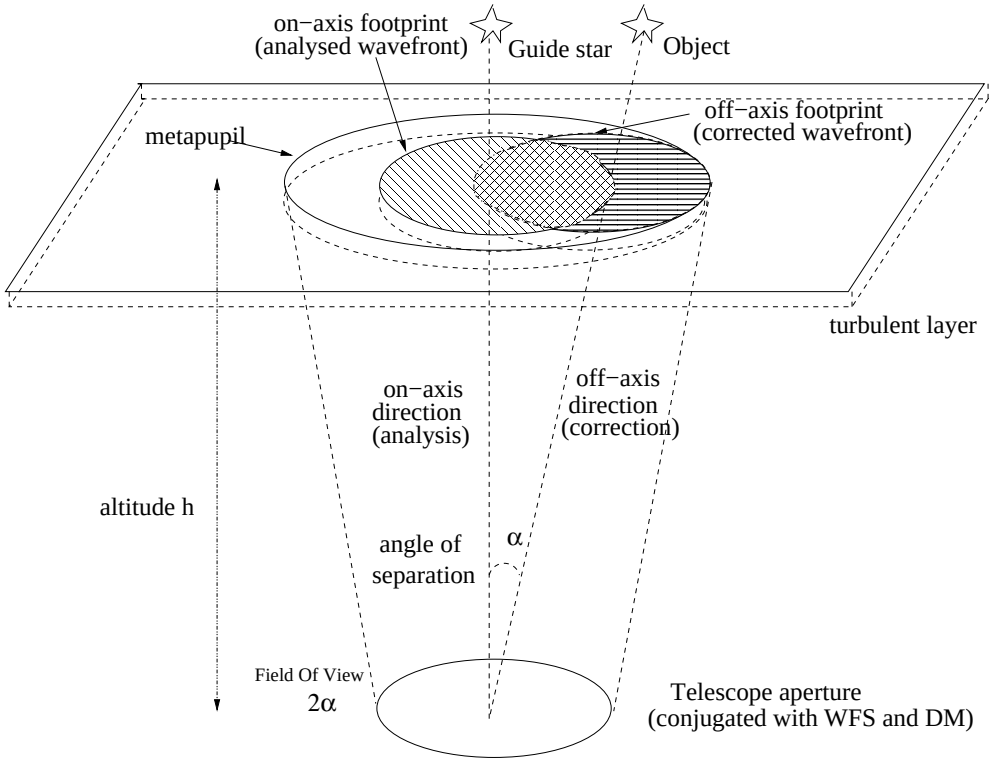

Figure 1. Principle of OAAO: we consider a single turbulent layer at altitude *h* and two stars with angular separation α. The projections of the entrance pupil in each direction define an on-axis (diagonal pattern) and an off-axis (horizontal pattern) footprint. The 2α FoV defines a metapupil encircling both footprints. OAAO consists in analyzing the on-axis turbulence to estimate the off-axis turbulent wavefront and correct it with a single DM conjugated with the aperture.

2.2. Open loop optimal control in OAAO

Considering a general open loop MCAO control problem, the optimality criterion consists in minimizing the mean residual phase variance (MMSE) in the FoV of interest.[3,4] OAAO is only a particular case of MCAO with a single direction of interest, then the problem comes down to the estimation of $\hat{\phi}(\mathbf{r},\alpha)$ minimizing the criterion:

$$\sigma_\alpha^2 = \varepsilon = \langle \| \hat{\phi}(\mathbf{r},\alpha) - \phi(\mathbf{r},\alpha) \|^2 \rangle_{\phi,noise}, \tag{1}$$

where $\langle . \rangle_{\phi,noise}$ stands for a mathematical expectation both on turbulence and detector noise, $\| . \|^2$ is a quadratic norm, $\phi(\mathbf{r},\alpha)$ is the true phase in the direction of interest α.

As long as we assume that noise and turbulence have Gaussian statistics and that the system is linear, an analytical expression of this estimator exists. Let $\mathbf{D}$ be the WFS measurement matrix, $\mathbf{P}_{gs}$ the projector of the phase of the metapupil (see Fig. 1.) on the on-axis footprint, $\mathbf{P}_\alpha$ the projector of the phase of the metapupil in the off-axis direction α, $\mathbf{C}_\phi$ the covariance matrix of the turbulent phase in the metapupil, $\mathbf{C}_n$ the slope noise covariance matrix. Then the optimal estimator can be written as a tomographic reconstruction in the metapupil ($\mathbf{W}_{tomo}$) followed by a projection in the direction of interest ($\mathbf{P}_\alpha$) in the form[4]:

$$\hat{\phi}(\mathbf{r},\alpha) = \mathbf{P}_\alpha \mathbf{W}_{tomo} \mathbf{s} = \mathbf{P}_\alpha \mathbf{C}_\phi (\mathbf{D}\mathbf{P}_{gs})^T ((\mathbf{D}\mathbf{P}_{gs}) \mathbf{C}_\phi (\mathbf{D}\mathbf{P}_{gs})^T + \mathbf{C}_n)^{-1} \mathbf{s}, \tag{2}$$

where **s** is the measured slope vector.
The last step of the control is to deduce the DM voltages **V** by a least square projection onto the DM subspace:

$$\mathbf{V} = ((\mathbf{M}^{DM})^T \mathbf{M}^{DM})^{\dagger} (\mathbf{M}^{DM})^T \hat{\phi} \tag{3}$$

where $\mathbf{M}^{DM}$ is the influence matrix defining the mirror modes and symbol † stands for the general inverse.
In the experiment, this MMSEE correction is compared to an open loop classic AO approach. In this case, the voltages $\mathbf{V}_{AO}$ are derived from the command matrix $\mathbf{M}_{com}$, general inverse of the experimental interaction matrix $\mathbf{M}^{int} = D\mathbf{M}^{DM}$, that is:

$$\mathbf{V}_{AO} = \mathbf{M}_{com}\mathbf{s} = ((\mathbf{M}^{int})^T \mathbf{M}^{int})^{\dagger} (\mathbf{M}^{int})^T \mathbf{s}. \tag{4}$$

Note that the experimental implementation of the MMSEE control requires to evaluate the matrices involved. We choose the Zernike mode basis to express the turbulent phases. In this context, $\mathbf{C}_{\phi}$ is the Noll matrix. $\mathbf{P}_{gs}$ and $\mathbf{P}_{\alpha}$ are easily computed from the geometrical configuration. **D** is deduced from a geometrical model of the Shack-Hartmann WFS and a calibration of the set-up. $\mathbf{M}^{DM}$ is derived from the experimental influence matrix of the DM. We assume a white uniform slope noise of variance σ_b^2, experimentally estimated. Then

$$\mathbf{C}_n = \sigma_b^2 \quad \mathbf{Id}, \tag{5}$$

where **Id** is the identity matrix.

3. EXPERIMENTAL VALIDATION OF MMSEE BASED OAAO

3.1. Experimental set-up description

OAAO tests have been performed thanks to the classic AO test bench BOA developed by ONERA. It is composed of a turbulence generator, a telescope simulator, the AO system and an imaging camera. The source is a fibered LASER diode working at $\lambda = 633$ *nm* placed on-axis. The turbulence generator is composed of a mirror placed in the collimated beam. It is assumed to reproduce a Kolmogorov spectrum with a $D/r_0 \simeq 3.6$ at 500 *nm*. A weak turbulence has been chosen for these first validations. More realistic turbulence should be simulated soon.

The wavefront corrector is based on a Tip Tilt Mirror (TTM) and a 9*9 actuator DM. The Shack-Hartmann WFS is composed of a 8*8 lenslet array and a 128*128 pixel DALSA camera (read out noise of $85e^-$/pixel/frame). The imaging camera is a 512*512 pixel Princeton camera (read out noise $4e^-$/pixel/frame). Note that this AO configuration is designed to work in closed loop, meaning the DM and TTM are placed before the WFS. In such a configuration, and without turbulence, the AO closed loop performance in terms of Strehl Ratio (SR) is about 73% (so called internal Strehl Ratio). Without correction but with turbulence, the SR is about 20%. Real Time Computing is performed at a 274Hz sampling rate with a NAOS like RTC based on C40 modules.

The AO configuration is modified for OAAO tests: a second source, identical to the first one, has been inserted. The two sources have a fixed angular separation $\alpha \simeq 50(\lambda/D)$ so that both sources can be imaged on the Princeton camera. A large pinhole is also placed in the entrance focal plan of the WFS so as to stop the light coming from the off-axis source.

To increase anisoplanatism effects, the turbulent mirror can be translated in altitude. Thus, the light beams from both sources intersect the turbulent layer defining two footprints, projection of the system aperture. The footprint relative separation δ is related to the altitude h, the angular separation α and the pupil diameter D by: $\delta = \alpha h/D$. Then, when the footprint relative separation δ increases from 0 to 40% on the set-up, it is equivalent to an angular separation between two stars ranking from 0 to 4 *arcmin* for an 8 meter telescope and a 3000 meter high turbulent layer. Note that the off-axis MMSEE matrix given in Eq. (2) has to be computed for each desired direction of interest. In the particular case of a null relative separation, the MMSEE matrix becomes an on-axis optimal reconstructor.

3.2. Description of the OAAO tests and results

The OAAO test protocol is the following. For each relative separation δ, the OAAO tests are performed in a static mode meaning on fixed occurrences of turbulence with the corresponding MMSE Estimator optimized in the off-axis direction. For each occurrence of turbulence the wavefront measurement and the correction are performed according to Eq. (2)-(3). So as to obtain statistical results, OAAO tests are performed on 15 occurrences of turbulence per relative separation and

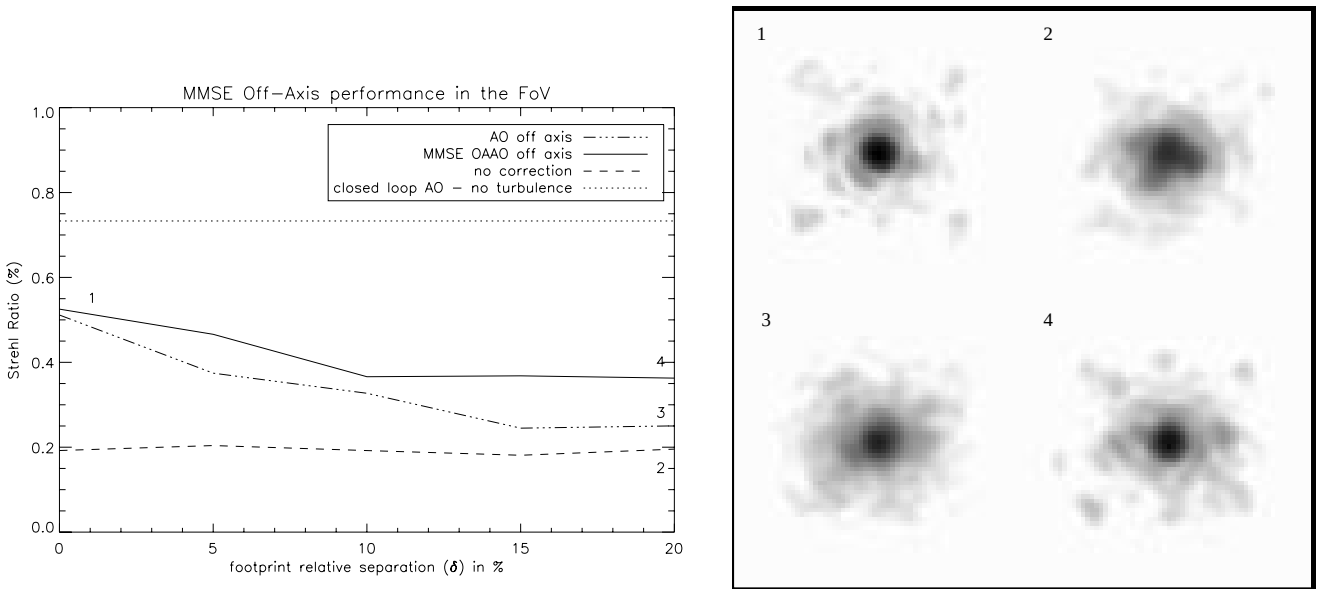

Figure 2. Left: OAAO performance on the off-axis star for different separations: solid line is off-axis MMSEE, dashed dotted line is open loop AO. No correction and closed loop AO with no turbulence SR are given as SR limits. Right: four experimental PSFs of the off-axis star are presented corresponding to: MMSEE correction at $\delta = 0\%$ (1) (no anisoplanatism), no correction (2), open loop AO correction at $\delta = 20\%$ (3), MMSE correction at $\delta = 20\%$ (4).

the resulting images are added up to compute long exposure images and to estimate the SR. Note that this protocol requires the DM to be flattened before slopes measurement using offset tensions. The applied voltages take into account this offset.

We also compare the experimental performance of MMSEE off-axis correction with the open loop AO correction (see Eq. (4)). The results of our first OAAO tests are presented in Fig.2. The left plot shows the evolution of the SR after correction, estimated from the experimental Point Spread Functions (PSFs), as a function of the footprint relative separation δ. The MMSEE off-axis optimization brings a clear improvement of the SR. The gain is also clearly seen on the long exposure PSFs also shown in the figure for four conditions of correction (see caption).

3.3. Comparison with numerical simulation and discussion of the experimental results

Using an end-to-end simulator dedicated to AO and MCAO simulation, an accurate numerical simulation of the OAAO experiment has been performed. This simulation includes the real influence matrix of the DM as measured by a Zygo interferometer, an accurate model of the Shack-Hartmann WFS, the one layer Kolmogorov turbulence. Every part of the experimental system has been reproduced according to calibrations so as to propose a reliable simulation of the set-up as described in Sect. 3.1 and provide expectable performance. A numerical simulation has been performed. It includes either a classic AO open loop reconstruction or an optimal off-axis reconstruction based on MMSEE as described before. As for the open loop OAAO experimental validation, performance have been measured for different footprint relative separation. In each case, the optimal control is adapted to the new separation so as to optimize the correction in the off-axis direction taking into account the open loop on-axis wavefront measurement, and the resulting off-axis SR is measured.

Fig. 3 shows the evolution of the performance of the MMSEE optimal control versus a classic AO correction as defined in Sect. 2.2. These numerical results can then be compared to the experimental ones. It clearly appears that even if the experimental results show indeed an improvement of the off-axis performance using MMSEE, this performance is nevertheless weaker than expected. Four points should be noted having regards to the experimental results compared to the numerical ones :

- the weak performance of both the classic AO and the MMSEE correction in the experiment for a null angular separation, compared to the numerical simulation ,

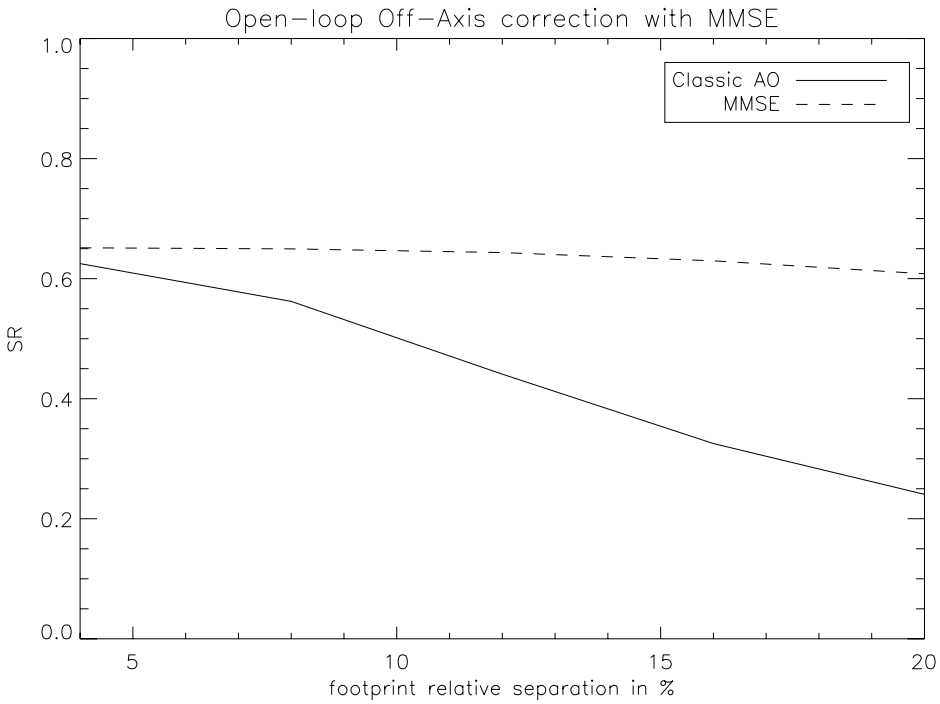

Figure 3. end-to-end simulation of the performance of a MMSE estimator optimal correction in the open-loop OAAO set-up configuration. The Strehl Ratio is given for the off-axis star according to the footprint relative separation in %. The solid line is the MMSE performance, the dashed line is obtained with classic AO control

- the higher experimental SR obtained for both correction for a $\delta = 20\%$ relative separation, corresponding to a 2 arcmin angular separation (still compared to simulation),
- the effect of anisoplanatism on the classic AO experimental correction seems rather quick (fast decorrelation),
- as said before, the performance of MMSEE is weaker in the experiment compared to the numerical simulation.

These elements lead us to question the quality of the turbulent phase screen. Recent measurements have indeed shown that the phase screen shows high frequency defects. These defects lead to a power excess in the high frequency spectrum, compared to the expected $D/r_0 \simeq 3.6$ Kolmogorov spectrum. Some other points are also currently being check, such as the the tip/tilt mirror position control, as a drift of this mirror has been observed in open loop. Static aberrations also introduce a bias in the estimation procedure and should be dealt with separately.

New tests should then be performed in the near future to check the improvement of the MMSEE optimal control in open loop OAAO when solving these problems. New phase screens have for instance been developed by Observatoire de Paris-Meudon and show better characteristics. Nevertheless, as our main goal is to demonstrate optimal control for closed loop OAAO, based on a Kalman filter, we are currently focusing on the implementation and testing of this configuration (See Sect. 4). Moreover, some of the problems encountered in open loop should be easily solved while working in closed loop.

4. KALMAN BASED CLOSED LOOP OAAO : EXPERIMENTAL IMPLEMENTATION AND NUMERICAL SIMULATION

It has been shown that MCAO finds its closed loop optimal control solution in a Kalman based control law. A full description of this control law can be found in[1] and more recent works on the subject in.[9,10] As for the open loop, the closed loop optimal control problem can be split into first an estimation problem, which solution is given by the Kalman filter, and a

command problem, simplified into a classic least square projection onto the DM modes. The OAAO configuration is well suited for an experimental validation of this solution. The optical set-up has been modified to perform real time, dynamic correction. The phase screen is now adapted to a rotating stage so as to reproduce the wind effects. The OAAO correction will then be realized dynamically, in closed-loop, with real time computing. We are currently implementing a new Real Time Computer (RTC) built by Shaktiware Inc., including a Kalman based optimal control for OAAO. It is based on a commercial Linux 1.8 GHz PC. According to benchmark tests, this new RTC should perform Kalman based correction up to a 500Hz sampling rate for 90 estimated modes, or a 130Hz sampling rate for 300 estimated modes. Currently, the sampling rate has been limited to 60Hz for a start.

The very first AO loop has been closed with a Kalman filter based control law. This is the very first time such an AO loop is closed as far as we know. This Kalman AO loop has been compared to a classic AO loop with an integrator (gain was 0.3 and close to the optimal). The conditions of experiment are close to the previous one, in terms of noise, turbulence level etc ..., but we use the new RTC with the 60 Hz sampling frequency and a wind speed V so that $V/D \simeq 0.3$. The SR obtained are 72% for the Kalman Filter and 70% for the integrator, which is close to the difference we could have expected according to the numerical simulation presented below (the SR error bar is about 1%). The corresponding PSFs measured with the imaging camera are shown on Fig.4. Now, this Kalman based AO loop needs to be studied in details. We will then focus on the closed loop off-axis correction.

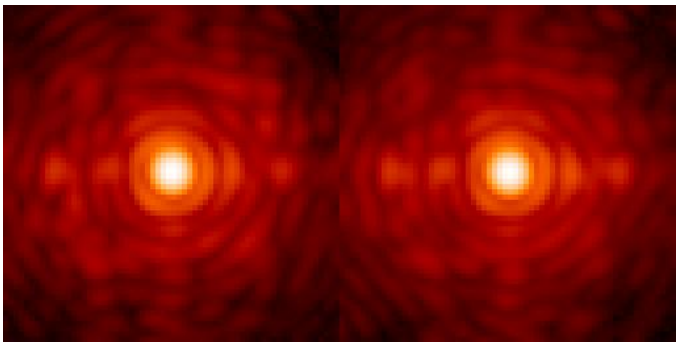

Figure 4. Comparison between the PSF obtained in a classic AO closed-loop configuration, first with a integrator (left) then with a Kalman based control (right). Log scale are used. Strehl Ratio are respectively 70% and 72%

As for the open loop OAAO validation, a numerical simulation of the expectable performance of the Kalman filter based closed loop OAAO can be performed. As previously, performance have been simulated thanks to the end-to-end simulator of the experimental set-up. The performance are measured for different footprint relative separations. In each case, the optimal control is adapted to the new separation so as to optimize the correction in the off-axis direction taking into account the closed loop on-axis wavefront measurement. Note that in this case the wind is in the direction defined by the two stars, the off-axis one being downstream.

Fig. 5 shows the evolution of the performance of the Kalman based optimal control versus a classic AO loop with a classic integrator controller. Thanks to the Kalman based control, the OAAO loop can be closed and the performance is found be equivalent to the open-loop MMSEE performance in the field of view. This simulation can be related to the expected performance of the Kalman filter in a full MCAO configuration as simulated in. [1]

5. KALMAN BASED OPTIMAL CONTROL : FIELD OF APPLICATION

The optimal Kalman based control has been proposed and developed in the MCAO context. Its advantage is to provide an optimal estimation of the phase in the volume which allows an efficient interpolation of the wave-front between the GSs

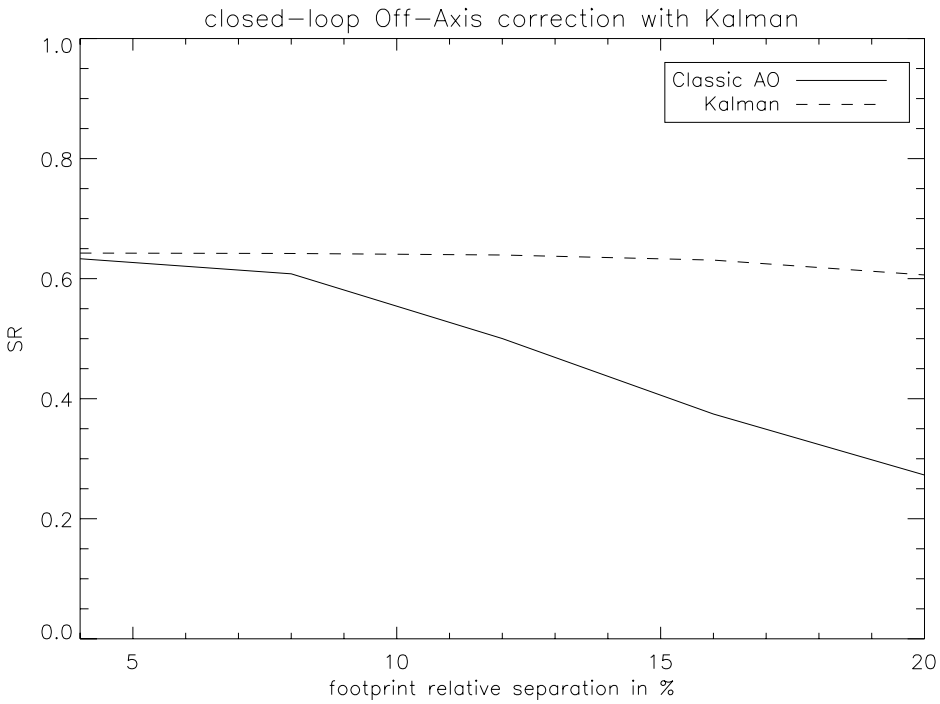

Figure 5. end-to-end simulation of the performance of a Kalman based optimal control in the closed-loop OAAO set-up configuration. The Strehl Ratio is given for the off-axis star according to the footprint relative separation in %. The solid line is the Kalman based control performance, the dashed line is obtained with a classic integrator

used for wave-front sensing. This estimation makes use of the available spatial and temporal priors (turbulence profile, temporal correlation). The correction commands are then deduced from the estimated phase by a projection onto the mirrors to optimize the correction in a specified FOV of interest.

The approach can be applied both to Laser GSs and Natural GS, to star and layer oriented [11] WFS. For a given system a significant gain is expected for extended FOVs.[1] Similarly for a given performance the optimal control can allow to reduce the system complexity (less or fainter GSs...).

The OAAO experiment presented here is a particularly demonstrative illustration in the simple case of a single GS and a single DM in the pupil correcting for a single direction of interest. Multiple Object Adaptive Optics (MOAO) is very similar to OAAO since it also consists in having a specific DM for each direction of interest. The only difference is that it uses several GSs for wave-front sensing. Besides, for extragalactic MOAO, such as the Falcon project, [12,13] the GSs are faint and far apart. All these elements make Kalman control especially attractive for this application.

The interest of our control approach for Ground Layer AO (GLAO) [14] could also be investigated. The specification of the FOV of interest could be helpful to improve the correction uniformity.

Finally, Kalman based control can also be of interest for classic AO. Although no significant improvement is expected when correcting only turbulence, the Kalman filter can easily account for vibrations.[9] In this case, performance can be highly improved compared to the standard integrator based control. This asset is all the more relevant for eXtreme AO (XAO).

6. CONCLUSION

We have proposed an original OAAO concept. This concept allows to test the reconstruction of the phase in the volume and the related optimal control issues with a simple hardware. OAAO experimental results have been obtained in open loop. The off-axis MMSE reconstructor confirms a clear gain compared to standard AO control. A recent end-to-end simulation of the system shows that a more significant improvement of performance should be obtained. Phase screen defects and

optimization of the experiment should allow an improvement of the overall performance. Nevertheless, these results constitute an encouraging first step toward MCAO optimal control, and now the effort is focused on closed-loop correction. For the first time, a classic AO loop has already been closed with a Kalman filter based control. And while a closed loop correction is currently being tested on the OAAO bench, simulations already indicate a very good correction in a large field of view. Experimental validation are so under progress.

7. KALMAN BASED CLOSED-LOOP OAAO: LATEST NEWS

As this article was being submitted, the first Kalman based OAAO loop has been closed. Here are the very first results obtained. The test has been performed in the same conditions as the experiments presented before. In particular, the dynamic conditions are those of the Kalman based closed loop AO test presented in Sect. 4. But the set-up has been slightly improved. The non common path aberrations have been compensated for so that without turbulence a classic AO loop closed with an integrator achieves a 87% internal SR. In this closed-loop OAAO test, a single footprint relative separation of 10% is considered. First, a classic AO loop has been closed with an integrator (gain was 0.5 and close to optimal). In this case, a very good correction is obtained on axis with a 84% SR, while the off-axis correction is only 55% SR due to anisoplanatism. Then, a Kalman based control has been applied so as to optimize the correction in the off-axis direction in closed-loop. The on-axis correction then decreases to 54% SR but the off-axis correction raises up to 64% SR. Fig. 6 shows the corresponding PSFs. The Kalman based closed-loop remained stable. This is the first Off-Axis correction performed in closed-loop with an optimal control. We still expect to improve these first results for instance with a better handling of static aberrations.

Figure 6. First Kalman based closed-loop OAAO test: these are PSFs in log scale obtained first with a standard integrator ($gain = 0.5$) (top), then with Kalman based optimal control for off-axis correction (bottom). Left-hand images are obtained for the on-axis star, right-hand images for the off-axis star. Note that images are originally separated by $50(\lambda/D) \simeq 190 pixels$ and have been brought closer for display

ACKNOWLEDGMENTS

The first author received a PhD grant from DGA, Ministère de la Défense, France. Part of this study has been supported by EC contract RII3-CT-2004-001566. The authors thank F. Mendez and B. Fleury for their fruitful help and P. Jagourel

and F. Hammer for their support.

REFERENCES

1. B. Le Roux, J.-M. Conan, C. Kulcsár, H.-F. Raynaud, L. M. Mugnier and T. Fusco, "Optimal control law for classical an multiconjugate adaptive optics", J. Opt. Soc. Am. A **21**, 1261-1276 (2004).
2. E. P. Wallner, "Optimal wave-front correction using slope measurements", J. Opt. Soc. Am. A **73**, 1771-1776 (1983).
3. B.L. Ellerbroek, "First-order performance evaluation of adaptive optics systems for atmospheric turbulence compensation in extended field of view astronomical telescopes", J. Opt. Soc. Am. A **11**, 783-805 (1994).
4. T. Fusco, J.-M Conan, G. Rousset, L.M. Mugnier and V. Michau, "Optimal wavefront reconstruction strategies for multiconjugate adaptive optics", J. Opt. Soc. Am. A **18**, (2001).
5. A. Knutsson, M. Owner-Petersen, "Emulation of dual-conjugate adaptive optics on an 8-m class telescope", Opt. Express **11**, (2003).
6. M. Langlois, C. D. Saunter, C. N. Dunlop, R. M. Myers and G. D. Love, "Multiconjugate adaptive optics : laboratory experience", Opt. Express **12**, (2004).
7. O. Von der Lühe, "Photometric Stability of Multi-conjugate Adaptive Optics", *Advancements in Adaptive Optics*, D. Bonaccini Calia, B.L. Ellerbroek, R. Ragazzoni , Proc. SPIE 5490, 2004
8. F. Quiros-Pacheco, C. Petit, J.-M. Conan, T. Fusco and E. Marchetti, "Control Law for the Multi-conjugated Adaptive Optics Demonstrator", *Advancements in Adaptive Optics*, D. Bonaccini Calia, B.L. Ellerbroek, R. Ragazzoni , Proc. SPIE 5490, (2004)
9. C. Petit, F. Quiros-Pacheco, J.-M. Conan, C. Kulcsár, H.-F. Raynaud, T. Fusco and G. Rousset, "Kalman Filter based control loop for Adaptive Optics" , *Advancements in Adaptive Optics*, D. Bonaccini Calia, B.L. Ellerbroek, R. Ragazzoni , Proc. SPIE 5490, (2004)
10. C. Kulcsár, H. F. Raynaud, C. Petit, J.-M. Conan, B. Le Roux, "Optimality, Observers and controllers in Adaptive Optics" , Proceedings of Optical Society of America, Charlotte, 2005
11. R. Ragazzoni, J. Farinato, E. Marchetti, "Adaptive optics for 100m class telescopes: new challenges require new solutions", Proc. SPIE 4007, p. 1076-1087, (2000)
12. F. Hammer, F. Sayède, E. Gendron, T. Fusco et al, "Scientific Drivers for ESO Future VLT/VLTI Instrumentation" , Proc. SPIE 139, 2001
13. F. Hammer, M. Puech, F. Assémat, E. Gendron, F. Sayède, P. Laporte, M. Marteaud, A. Liotard, F. Zamkotsian, "Second Workshop on ELT" , Proc. SPIE 5382, 727, 2004
14. F. Rigaut, "Ground-conjugate wide field adaptive optics for the ELTs" , Astronomical Observatory of Padova, Beyond Conventional Adaptive Optics, E. Vernet, R. Ragazzoni and S. Esposito, Padova, Italy, Proc. ESO , 58, (2001)